Gas and Solids Behavior in a Baffled and Unbaffled Slurry Bubble Column

New data and analyses are presented for describing gas and solids behavior in a slurry bubble column. Axial solids concentration and bubble size distributions were measured in a 0.108 m ID slurry bubble column apparatus operated at steady state conditions. The column was operated with and without internal baffles. The slurry and gas superficial velocities ranged from 0.0077 to 0.009 m/s and from 0.031 to 0.24 m/s, respectively. The solid phase consisted of glass spheres in a narrow size range with a mean diameter of 96.5 μm; the liquid phase consisted of tap water.

With a one-dimensional sedimentation-dispersion model, the data have been used to predict average solids loadings and axial distributions of the solids for specified operating conditions. Local bubble size and concentration measurements indicate that the slurry bubble column was operated in the churn-turbulent flow regime throughout the entire range of operating conditions used in this study. The impact of internal baffles and solids concentration on the gas and solids behavior is discussed.

W. O'Dowd, D. N. Smith, J. A. Ruether
Pittsburgh Energy Technology Center
Pittsburgh, PA 15236

S. C. Saxena
Department of Chemical Engineering
University of Illinois
Chicago, IL 60680

Introduction

The slurry bubble column reactor is widely used in the hydroprocessing and fermentation industries and has been the subject of active research for more than two decades. Generally, the slurry bubble column reactor is run in either the semibatch mode or the continuous mode of operation, in which gas is bubbled continuously through either a stationary or a flowing slurry. Several variations of the basic slurry bubble column have been investigated to improve performance and to extend the range of operating conditions (Muroyama et al., 1985; Fajner et al., 1985; Tanaka et al., 1984; Kato et al., 1982). These investigations have focused on the hydrodynamic behavior of a three-phase system in multistage and draft tube slurry bubble columns. The primary purpose of devising these modifications of a slurry bubble column was to either decrease slurry mixing or increase gas holdup.

In the present investigation, the effect of vertically suspended rods on the hydrodynamics in a slurry bubble column has been investigated. This modification to the basic slurry bubble column is important for exothermic reactions that require considerable heat removal (Kölbel and Ralek, 1980; Deckwer et al., 1982; Shah et al., 1982). The hydrodynamic parameters that have been investigated are the bubble size, gas holdup, solids dispersion coefficient, and hindered settling velocity. The experimental conditions were adjusted so that the churn-turbulent flow regime was achieved. This flow regime is most likely to occur in scaled-up slurry bubble column reactors.

Previous investigations of hydrodynamics in a slurry bubble column have rarely measured bubble size (Shah et al., 1985a; Smith et al., 1984; Kato et al., 1973), even though this hydrodynamic parameters is of utmost importance for determining mass transfer to accomplish reliable design and scale-up (Heijner and van't Riet, 1984).

In this paper, new data for slurry bubble column operation with and without baffles are presented for hydrodynamic parameters that describe gas and solids behavior. A one-dimensional sedimentation-dispersion model is used to describe axial solids concentration distributions. The approach of Nicklin (1962) is used to describe gas holdup. The drift velocity for the churn-turbulent flow regime is defined as the sum of the superficial gas velocity and terminal bubble rise velocity as proposed by Towell et al. (1965).

Experimental Method

A schematic of the slurry bubble column apparatus is shown in Figure 1. The bubble column is a transparent acrylic cylinder

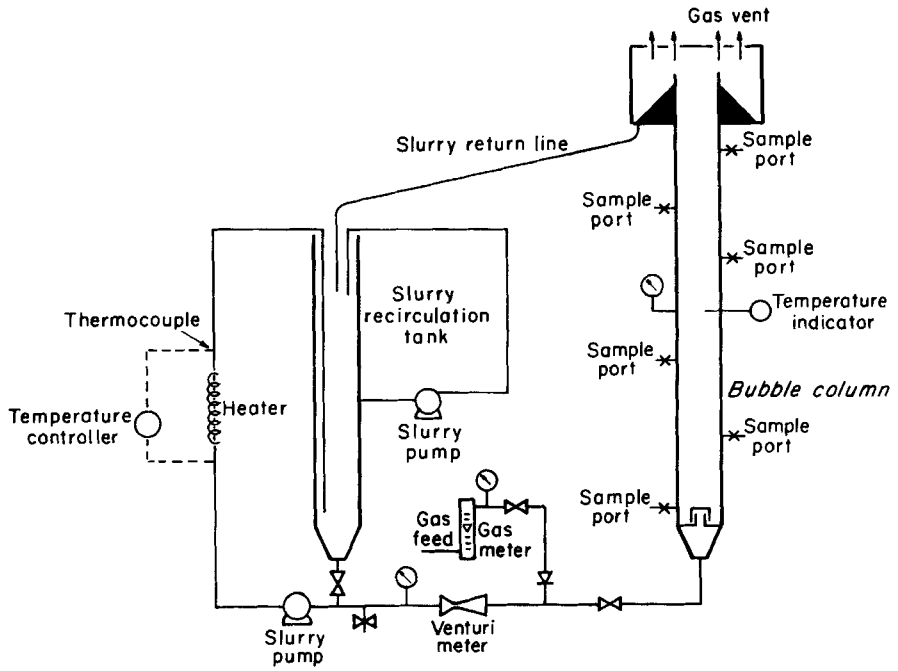

Figure 1. Slurry bubble column apparatus.

of 0.108 m dia. and 1.94 m length. The system was operated in the continuous mode, with the slurry from a recirculation tank pumped into the column by a progressive cavity pump. The gas and slurry mixture entered at the bottom of the column through a perforated plate that consisted of 72 holes of 0.001 m dia.

Experiments were conducted at steady state flow with the gas superficial velocity ranging from 0.031 to 0.24 m/s and with the slurry superficial velocity maintained constant at 0.0077 and 0.009 m/s for the unbaffled column and the baffled column, respectively. Details of the slurry bubble column and other associated components have been discussed previously (Smith and Ruether, 1985).

Details of the internal baffles and their arrangement in the bubble column are shown in Figure 2. The baffles were suspended from the top of the column and consisted of five vertically arranged Plexiglas rods that were 0.019 m in dia. and 1.88 m high.

The solid, liquid, and gas phases were respectively monodisperse glass spheres, water, and nitrogen. The glass spheres had a particle size range between 88 and 105 μm and a density of 2,420 kg/m^3. The axial solids concentration distribution was determined from six slurry-sampling ports that were vertically spaced at intervals of 0.35 m, with the first port located at 0.0405 m above the distribution plate. All six samples were taken simultaneously with electronically actuated sample valves.

Local *in situ* gas-holdup and bubble-size measurements were performed using a dual conductivity probe and an integrated data acquisition and analysis system. The conductivity probe consisted of two Teflon-coated 0.076 mm dia. chromel wires. The data acquisition system consisted of a multichannel waveform recorder, which is an analog-to-digital converter with a solid-state memory, and an IBM PC computer, which was used to control the acquisition of data and to store data from the waveform recorder. A detailed description of the conductivity probe and the associated data acquisition system is given by Smith et al. (1984).

Analysis of gas phase

Two important quantities need to be determined from the response of the conductivity probe: the dwell time on each probe, and the lag time associated with the bubble while traversing the axial gap between each probe. The dwell time τ corresponds to the duration of time the gas bubble is in contact with the probe, whereas the lag time ΔT is computed from the time interval it

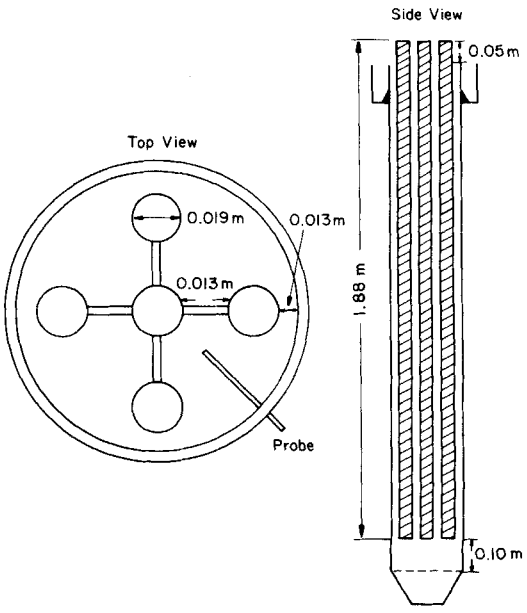

Figure 2. Details of internal baffles and their arrangement.

takes for the centroid of the bubble to pass from the upstream to the downstream probe. To determine when a gas bubble is in contract with the probe, a slope method similar to that of Burgess and Calderbank (1975) was used. A description of the slope method has been given previously by Shah et al. (1985b).

The local gas holdup was determined by summing the dwell times for the gas bubbles and dividing by the total sample time. The bubble chord lengths were determined by Eq. 1 for a matched signal pair.

$$\lambda = \frac{h\tau}{\Delta T} \tag{1}$$

Matching the signal pairs required that several conditions be satisfied. The difference in dwell time between a signal pair must be within 30% of the dwell time on each probe, and the ascending velocity of the bubble must be between 0.05 and 1.70 m/s. An example of the direct signal and a detailed description of the interpretation of the response from a dual conductivity probe has been given previously by Fuchs and Smith (1982).

The gas holdup and bubble lengths were determined at four radial positions and three axial heights. The power law model was used to describe the radial profiles for both the gas holdup and bubble lengths, and is given by Eqs. 2 and 3, respectively.

$$\epsilon_g(r^*) = \epsilon_{g_c}(1 - r^{*N}) \tag{2}$$

$$\lambda(r^*) = (\lambda_c - \lambda_w)(1 - r^{*M}) + \lambda_w \tag{3}$$

The gas holdup at the wall is set equal to zero, which is a common assumption used to describe the radial gas holdup profile (Walters and Blanch, 1983; Ueyama and Miyauchi, 1979) and has been validated by previous experiments (Nassos and Bankoff, 1966; Hills, 1974). The effective radius R of the baffled column is the distance between the outer surface of the center rod and the column wall. The effective radial position of the probe in the baffled column was referenced from the outer surface of the center rod ($r^* = 0$). The effective diameter of the column is based on the free cross-sectional area, Eq. 4, where n is the number of rods ($n = 5$ for a baffled column; $n = 0$ for an unbaffled column).

$$D = \sqrt{(0.108)^2 - nD_r^2} \tag{4}$$

The bubble size is of importance in the determination of the mass transfer resistance in a bubble column. The bubble lengths, obtained from the conductivity probe, were interpreted according to the probability model suggested by Tsutsui and Miyauchi (1980). A log normal distribution of bubble sizes was assumed and the probability factors used to interpret the relationship between bubble size and bubble length have been given by Hess (1983). Previously, derivations by Werther (1974) and Ueyama and Miyauchi (1979) as well as experimental investigations by Yamashita et al. (1979) and Smith et al. (1984) have shown that the relationship between bubble length and the Sauter mean bubble size is described by Eq. 5.

$$d_{vs} = 1.5\bar{\lambda} \tag{5}$$

The average gas holdup was determined by integrating the power law fit over the column radius. The average bubble size was determined by volume-averaging the power law fit for bubble length over the column radius, Eq. 6.

$$\bar{d}_{vs} = \frac{1.5\int_o^1 r^*\epsilon_g(r^*)\lambda(r^*)dr^*}{\int_o^1 r^*\epsilon_g(r^*)dr^*} \tag{6}$$

Interfacial area was determined from the average bubble size and gas holdup, Eq. 7.

$$a = \frac{6\epsilon_g}{\bar{d}_{vs}} \tag{7}$$

Here, $\bar{d}_{vs}$ is obtained from the average bubble size of the three axial positions, and the holdup is determined experimentally from the height differential between the aerated and stagnant slurry.

Analysis of solids behavior

The solids concentration distribution in a cocurrent upward-flow slurry bubble column operated at steady state conditions appear to be well described by a one-dimensional sedimentation-dispersion model (Smith and Ruether, 1985). The mass balance of solids as a function of axial position in the column is the following:

$$\frac{E_s}{L}\frac{dC_s}{dX} + \left[\frac{U_{sL}}{(1-\epsilon_g)} - \bar{\psi}_L U_p\right] C_s = U'_{sL} C_s^f \tag{8}$$

The assumptions used in deriving Eq. 8 are that the slurry bubble column operates at steady state conditions; the gas holdup does not vary significantly with axial position; and the fraction of liquid in the slurry is assumed to be independent of axial position and is to be given as a function of average solids concentration in the column. If the solids concentration at the top of the column is defined as C_s^1, integrating Eq. 8 gives the following expression:

$$C_s = \left(C_s^1 + \frac{U'_{sL}C_s^f}{\bar{\psi}_L U_p - U_{sL}}\right)\exp\left[\frac{(\bar{\psi}_L U_p - U'_{sL})L(1-X)}{E_s}\right] - \frac{U'_{sL}C_s^f}{\bar{\psi}_L U_p - U'_{sL}} \tag{9}$$

Nonlinear least-squares regression was used to compute the values of C_s^1, U_p, and E_s for each solids concentration profile measured. For each computation, six measured slurry concentrations were used, and the values of the three parameters were determined to minimize the residual sum of the squares between the observed and calculated solids concentration using Eq. 9. The objective function employed was

$$F = \sum_{i=1}^{6} [C_s(\text{calculated}) - C_s(\text{observed})]_i^2 \tag{10}$$

A search model described by Ahrendts and Baehr (1981) was used to obtain the minimum value of F.

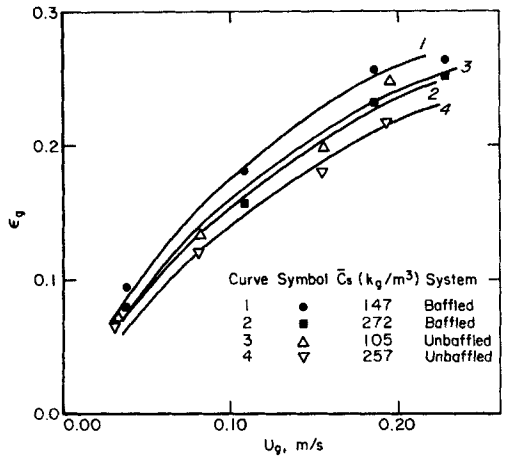

Figure 3. Average gas holdups vs. superficial gas velocity.

Gas Phase Results

The aim of the present studies was to investigate the effect of baffles on the gas phase characteristics in a slurry bubble column operated in the churn-turbulent flow regime. The average as well as the local gas holdup and bubble size, measured by an *in situ* conductivity probe, were determined for a narrow range of solids loading. The experimental results indicate that gas holdup, bubble size, and interfacial area are dependent upon the presence of baffles.

Gas holdup

Gas holdup data showing the effect of the operating parameters are displayed in Figure 3. The average gas holdup was larger in a baffled column than in an unbaffled column at comparable operating conditions, although the difference is within the error associated with the experimental measuring technique. Shah et al. (1978) reported that there was not an appreciable effect of vertical cylindrical baffles (up to 25% of column volume) on the gas holdup in a two-phase bubble column (0.0635 m ID). Without further investigation, this discrepancy between the results of the two studies cannot be satisfactorily explained. However, this discrepancy possibly could be attributed to different baffle arrangements or the difference in column diameter, which could effect the flow regime present.

Also, increasing the solids concentration results in a decreasing gas holdup for both the baffled and the unbaffled column. Previous studies (Kara et al., 1982; Roy et al., 1963; Koide et al., 1984; Capuder and Koloini, 1984; Ying et al., 1980) reported similar results for increasing solids loading on gas holdup in unbaffled slurry bubble columns. Decreasing gas holdup is related to the increased coalescence of bubbles. It is suggested that the increased coalescence results from increased viscosity because all relevant physical properties, except slurry density, do not change with increased solid concentration.

Modeling of the gas holdup is based on the Nicklin (1962) approach, Eq. 11, which describes the gas holdup to be dependent upon the superficial gas velocity, the superficial slurry velocity, and the drift velocity.

$$\epsilon_g = \frac{U_g}{U_g + U_{sL} + U_o} \tag{11}$$

The drift velocity for the churn-turbulent flow regime is assumed to be equal to the superficial gas velocity and the characteristic terminal rise velocity of the swarm of bubbles, Eq. 12.

$$U_o = U_g + U_{b\infty} \tag{12}$$

Inserting Eq. 12 into Eq. 11 results in Eq. 13.

$$\epsilon_g = \frac{U_g}{2U_g + U_{sL} + U_{b\infty}} \tag{13}$$

Equation 13 is used to model the systems investigated in this study.

The gas holdup is determined by the differential height method. With known values of the gas and slurry superficial velocities, the unknown parameter, $U_{b\infty}$, is determined from Eq. 13. For a system with constant operating conditions (type of solids, solids loading, type of liquid, column configuration, etc.) the terminal rise velocity is assumed to be independent of gas superficial velocity in the fully developed churn-turbulent flow regime. The parity plot of the calculated gas holdup, using an average terminal rise velocity, vs. the experimental holdup is shown in Figure 4 along with the average terminal rise velocity.

The terminal rise velocity reflects the bubble size distribution that is present. Terminal rise velocities shown in Figure 4 indicate, according to Haberman and Morton (1953) and Peebles and Garber (1953), that large bubbles (having a large equivalent diameter) are present. To accurately describe the characteristic terminal rise velocity from the bubble size distribution, not only requires the distribution of the bubble size but also the shape factor. This type of analysis is beyond the scope of this work.

Local gas holdups and the resulting fit to the power law model, Eq. 2, are shown in Figures 5 and 6 for the unbaffled and baffled column, respectively. The resulting fit is shown to agree reasonably well, which has also been shown in previous studies (Nassas and Bankoff, 1966; van der Welle, 1985). In Figure 7, a parity plot is shown for the average gas holdup determined by the differential height and the integration of the local gas holdup values. The holdups determined by averaging the local values are shown to be 13% less than the holdups obtained from the differential height measurements.

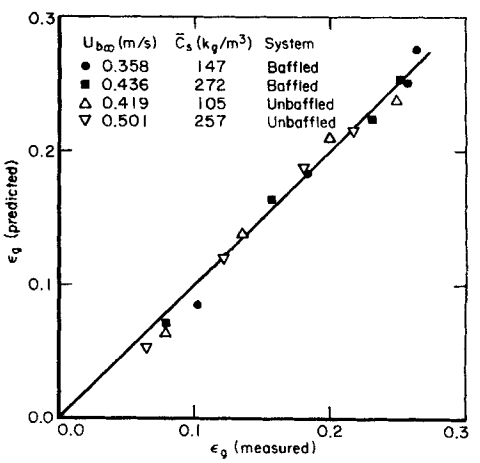

Figure 4. Parity plot for gas holdup.

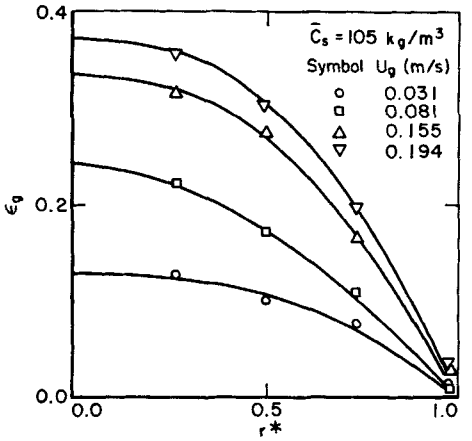

Figure 5. Holdup profiles for a slurry bubble column without baffles.

The radial distribution of gas holdup is an indicator of the extent of mixing of the liquid (Hills, 1974; Walters and Blanch, 1983; Ueyama and Miyauchi, 1979). Walters and Blanch developed a model to quantify the dispersion coefficient from the radial holdup profile. The liquid dispersion obtained from the Walters and Blanch model is within 18% of the solids dispersion coefficient obtained from Eq. 21. It has been reported by Kato et al. (1972) that the solids dispersion is proportional to that of liquid at small particle Reynolds numbers. Kato et al. and Joshi (1980) reported correlations that predict the dispersion coefficient in slurry bubble columns. The liquid dispersion coefficients obtained from correlations by Kato et al. and Joshi (excluding U_g = 0.031 m/s) are within 30% and 14%, respectively, of the solids dispersion coefficient, Eq. 21, determined in this investigation. The above correlations for liquid dispersion (Joshi, 1980; Kato et al., 1972; Walters and Blanch, 1983) apply to unbaffled bubble columns so a direct comparison of the local holdups using the model of Walters and Blanch is not possible. It has been speculated by Walters and Blanch and more recently by Heijner and van't Riet (1984) that holdups are strongly influenced by

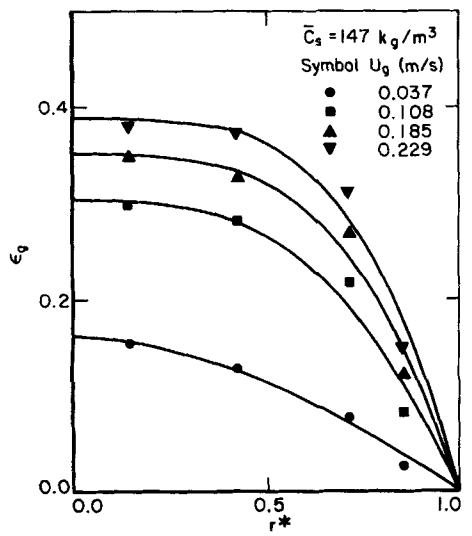

Figure 6. Holdup profiles for a slurry bubble column with baffles.

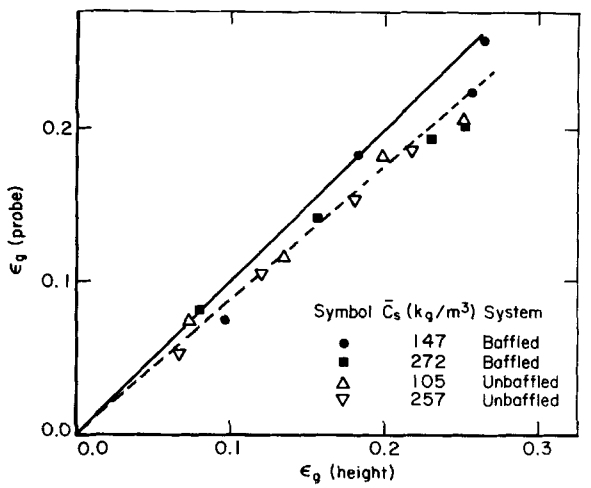

Figure 7. Average holdup obtained from conducting probe vs. height differential method.

the mixing, which may be a possible explanation for increasing holdup in the presence of baffles, but would seem to be contradicted by the holdup results of Shah et al. (1978).

Bubble size

The churn-turbulent flow regime is characterized by large bubbles occupying the center annulus, with smaller bubbles existing in the wall region. The radial distribution of Sauter mean diameter for both the unbaffled and baffled column are shown in Figures 8 and 9, respectively. The average Sauter mean bubble diameters, obtained from Eq. 6, for all the measurements are shown in Figure 10. Clearly, the presence of baffles alters the behavior of the measured Sauter diameter, as each column configuration shows a similar behavior with gas velocity.

The Sauter mean bubble size in the unbaffled column shows a maximum at a gas velocity of 0.081 m/s for both solid concentrations, 147 and 257 kg/m³, and remains relatively constant for the other gas velocities investigated. Sauter mean bubble sizes in the baffled column increase with increasing gas velocity and can be described by Eqs. 14 and 15 for solids concentrations of 147 and 257 kg/m³, respectively.

$$d_{vs} = 0.019\, U_g^{0.19} \tag{14}$$

$$d_{vs} = 0.023\, U_g^{0.23} \tag{15}$$

At low gas velocities, the bubble size that was measured in the baffled column is smaller than the bubble size in the unbaffled column, and at high gas velocities, larger bubble sizes were measured in the baffled column compared to the unbaffled column. This was not expected from the holdup results previously discussed, and may be a reflection of the experimental technique of measuring local bubble size and holdup in the free volume between baffles.

The Sauter diameter increases with solids loading for the baffled and unbaffled column. The increased bubble size is associated with increased viscosity, which promotes coalescence. The larger bubbles are associated with increased terminal rise velocities for the churn-turbulent flow regime. A relationship

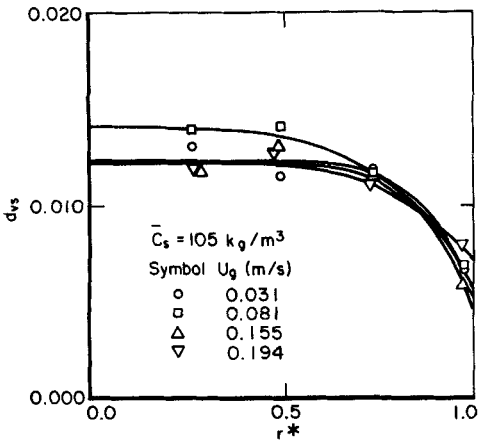

Figure 8. Bubble size profiles in an unbaffled slurry bubble column.

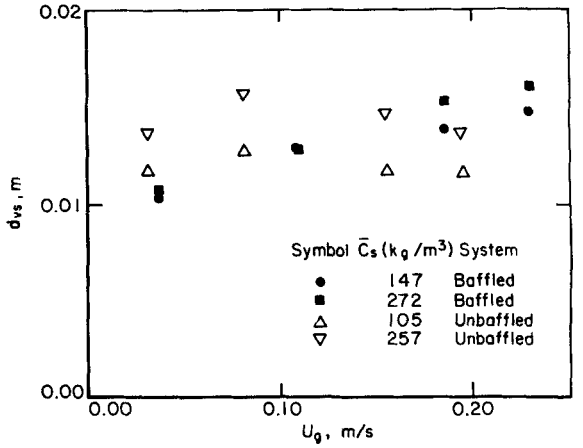

Figure 10. Bubble size vs. superficial gas velocity.

between Sauter mean diameter and gas holdup (or rise velocity) is expected to be established if the variance in the bubble size distribution remains the same and only the geometric mean bubble size varies. However, in a more general sense, the gas holdup is more nearly quantified by taking into account the cumulative bubble size distribution and the associated fraction of gas volume related to a narrow range of bubble size. Integration of the fraction of bubbles traveling at their terminal rise velocity should be compared directly with those determined from Eq. 13 and shown in Figure 4.

The cumulative frequency distribution of bubble sizes at one local position in the unbaffled column over the range of gas velocities investigated is shown in Figure 11. In general, trends are established for the behavior of bubble size distributions: The variance of cumulative frequency distribution increases with increasing gas velocity until 0.155 m/s and then becomes insensitive to a further increase in gas velocity. Increasing solids loading decreases the variance and increases the geometric mean bubble diameter for both the unbaffled column and the baffled column. The population of small bubbles can be significant, indicating that the two-bubble-class model (Shah et al., 1985a) may be applicable.

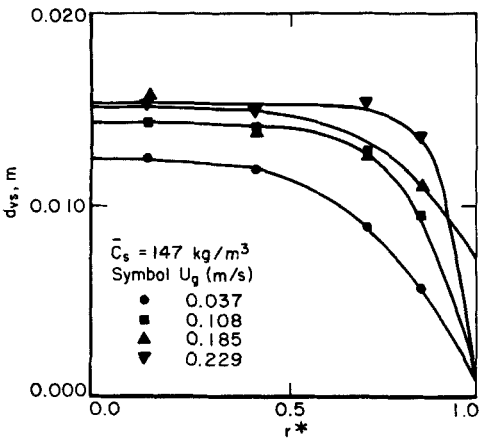

Figure 9. Bubble size profiles in a baffled slurry bubble column.

Interfacial area

The gas phase interfacial area, described by Eq. 7, is a function of the gas holdup and bubble size that exist in the slurry environment. Bubble size and gas holdup have both been shown to be sensitive to gas velocity, solids loading, and column configuration.

The range of solids concentration investigated was small, therefore the interfacial area was correlated only with the superficial gas velocity. The resulting equations are given for the baffled column.

$$a = 1.95\, U_g^{0.37} \tag{16}$$

$$a = 1.72\, U_g^{0.40} \tag{17}$$

and for the unbaffled column:

$$a = 4.17\, U_g^{0.74} \tag{18}$$

$$a = 2.95\, U_g^{0.71} \tag{19}$$

at 10 and 20 wt. % solids loading, respectively.

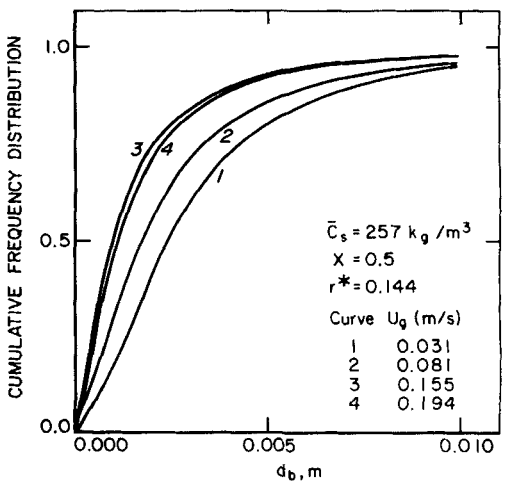

Figure 11. Cumulative frequency distribution of bubble size in an unbaffled slurry bubble column.

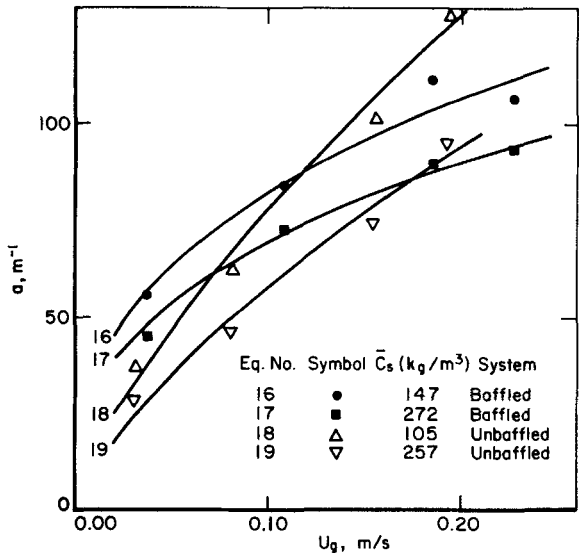

Figure 12. Interfacial area vs. superficial gas velocity.

The interfacial area calculated from Eqs. 16–19 and the measured interfacial area are shown in Figure 12. At low gas velocities the interfacial area is greater in the baffled column, while at higher gas velocities the reverse is true. While there have not been previous investigations into the effect of a vertical baffle arrangement on the interfacial area, there have been numerous investigations in unbaffled slurry columns. Quicker et al. (1984) investigated the effect of three different solids on interfacial area and reported the following correlation:

$$a = 0.140\, U_g^{0.81}\, U_{sL}^{-0.22} \tag{20}$$

The effect of gas velocity, Eqs. 18 and 19, from the present study is in reasonably good agreement with that of Quicker et al. The operating conditions are shown along with the measured gas phase characteristics in Table 1.

Solid Phase Results

To completely describe axial solids concentration distributions in a slurry bubble column, expressions for the solids concentrations at the top of the column, the hindered settling velocity, and the solids dispersion coefficients must be developed. In the following, the dependence of these three parameters on independent operating variables is evaluated over the range of experimental conditions used in this study. Finally, a comparison is made between the measured and predicted axial solids concentration distributions from the correlated parameters and sedimentation-dispersion model.

Hindered settling velocity

In general, operating variables that influence the hindered settling velocity, U_p, are thought to include the superficial gas velocity, average solids concentration, and terminal particle velocity (Kato et al., 1972; Smith and Ruether, 1985; Smith et al., 1986). Since the terminal velocity was not varied in this study (U_t = 0.0077 m/s), the dependence of U_p and U_t described

Table 1. Gas Phase Results

				Power Law Fit			
Run No.	System	U_g	C_s	ϵ_{gc}	N	d_{vs}	a
R1	Baff.	0.037	246	0.151	2.74	0.0107	44.9
R2	Baff.	0.108	263	0.301	1.78	0.0128	73.0
R3	Baff.	0.185	289	0.330	2.82	0.0155	89.5
R4	Baff.	0.229	288	0.393	2.11	0.0161	93.8
R5	Baff.	0.037	156	0.162	1.75	0.0103	55.9
R6	Baff.	0.108	147	0.304	3.03	0.0130	84.1
R7	Baff.	0.185	141	0.352	3.55	0.0138	111.7
R8	Baff.	0.229	143	0.389	3.94	0.0148	106.7
Z1	Unbaff.	0.031	101	0.131	2.62	0.0118	36.6
Z2	Unbaff.	0.081	107	0.244	1.84	0.0128	62.9
Z3	Unbaff.	0.155	104	0.337	2.34	0.0117	101.6
Z4	Unbaff.	0.194	109	0.373	2.51	0.0116	128.6
Z5	Unbaff.	0.031	270	0.138	1.31	0.0137	28.8
Z6	Unbaff.	0.081	259	0.212	2.03	0.0158	46.3
Z7	Unbaff.	0.155	260	0.311	1.95	0.0147	74.1
Z8	Unbaff.	0.194	237	0.356	2.20	0.0138	95.1

by Smith and Ruether (1985) was used in developing a correlation. A regression analysis of the hindered settling velocity on operating variables has given the following equations for baffled and unbaffled columns. For the baffled column,

$$U_p = 1.86\, U_g^{0.30}\, U_t^{0.80} \bar{\psi}_L^{3.5} \tag{21}$$

and for the unbaffled column,

$$U_p = 1.69\, U_g^{0.23}\, U_t^{0.80} \bar{\psi}_L^{1.28} \tag{22}$$

The values of hindered settling velocity predicted by Eq. 22 for an unbaffled column are in good agreement with those predicted by Kato et al. (1972) and Smith and Ruether (1985). The expression for the hindered settling velocity in the paper of Smith and Ruether has two errors: the coefficient after the

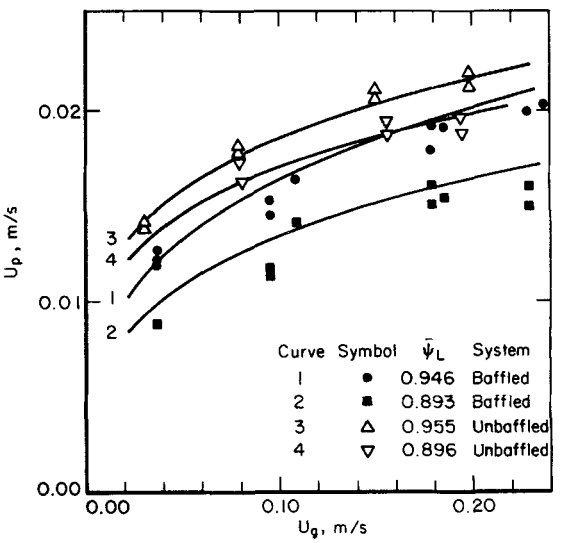

Figure 13. Hindered settling velocity vs. gas velocity for unbaffled and baffled columns.

equality sign should be 1.91 instead of 1.10; and the power dependency for superficial gas velocity should be 0.26 instead of 0.026. The dependence of hindered settling velocity on the liquid fraction in the slurry is relatively small compared to that reported in the literature (Kato et al., 1972; Smith and Ruether, 1985) and this may be due to the limited range investigated. The dependence of hindered settling velocity on gas velocity is similar to that reported in the literature and is shown in Figure 13. Equations 21 and 22 are for a limited solids investigation and should be seen as being more provisional in nature than a more complete investigation of solids behavior such as that by Smith and Ruether (1985).

The hindered settling velocity decreases by approximately 15% when baffles are present in the column and all other operating conditions are the same. This change in hindered settling velocity cannot be interpreted at the present time but may be related to the increase in wall surface area with the baffles present, which could increase the drag resistance of fluids in the column, thereby lowering the hindered settling velocity.

Solids dispersion coefficient

Axial solids backmixing or dispersion is characteristic of slurry bubble columns. Increased turbulence of the slurry is induced in the slurry from the wakes of bubbles. The rate of dispersion of solids has been shown to be proportional to the rate of dispersion of liquid and to approach liquid dispersion behavior for small-particle Reynolds numbers (Kato et al., 1972). The measured solids dispersion coefficients for the unbaffled column and the baffled column are shown in Figure 14 for the range of gas velocities used in this study. The effect of the liquid fraction in the slurry on the solids dispersion coefficient can be considered negligible for the baffled column, and only a slight dependence is observed for the unbaffled column. A quantitative description of the solids dispersion coefficient is generally expressed in terms of a solids Peclet number. A regression analysis of the solids Peclet number as a function of the Froude number, gas Reynolds number, and particle Reynolds number similar to the expression developed by Riquarts (1981) gives the following expressions. For the baffled column,

$$Pe_p = 7.4(Fr_g^6/Re_g)^{0.115} + 0.019\, Re_p^{1.1} \qquad (23)$$

and for the unbaffled column,

$$Pe_p = 7.7(Fr_g^6/Re_g)^{0.098} + 0.019\, Re_p^{1.1} \qquad (24)$$

Since Re_p was not varied in the present study, the coefficients for Re_p suggested by Smith and Ruether (1985) were used in Eqs. 23 and 24. Comparison of Eqs. 23 and 24 reveals that the solids dispersion coefficient is larger for the baffled column than for the unbaffled column, This indicates that the presence of baffles increases the intensity of solids mixing. In general, the ratio U_p/E_s is larger for the unbaffled column than for the baffled column. The phenomenon of increasing hindered settling velocity with decreasing solids dispersion coefficient in a variety of liquid mixture system, at otherwise similar operating conditions, has also been observed by Badgujar et al. (1986).

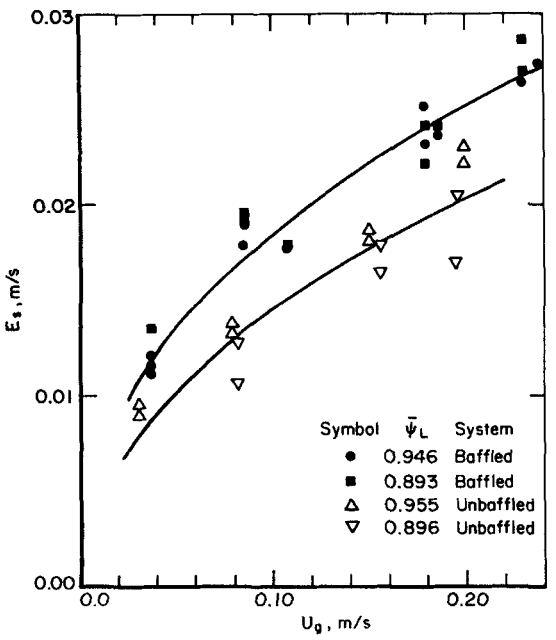

Figure 14. Dispersion coefficient vs. gas velocity for unbaffled and baffled columns.

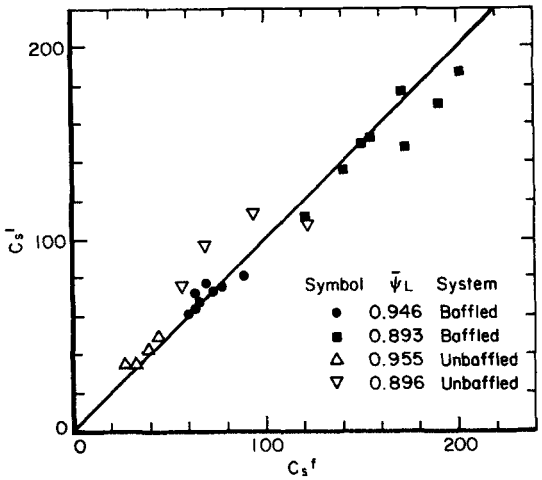

Figure 15. Solids concentration leaving column vs. feed concentration.

Solids concentration at top of column

The boundary conditions for the description of the solids concentration distribution in a slurry bubble column have been a point of controversy for several years (Cova, 1966; Yamanaka et al., 1970; Suganuma and Yamanishi, 1966; Kato et al., 1972; Smith and Ruether, 1985; Smith et al., 1986). Cova and Yamanaka et al. held that the solids concentration at the top of the column is the same as the effluent or feed concentration. Others have reasoned that the solids concentration at the top of the column does not necessarily equal the effluent solids concentration.

The solids used in the present study are a subgroup of the solids used by Smith and Ruether (1985), who showed that the solids concentration at the top of the column, C_s^l, was 27% larger than the feed solids concentration, C_s^f. A regression analysis on C_s^l as a function of C_s^f for all solids data of the present study in the unbaffled column shows that C_s^l is 8% higher than C_s^f. However, a similar analysis that excludes a single datum, possibly an

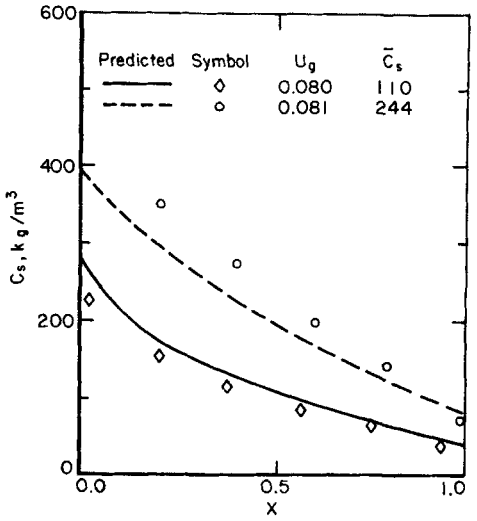

Figure 16. Axial solids concentration as a function of solids loading (unbaffled column).

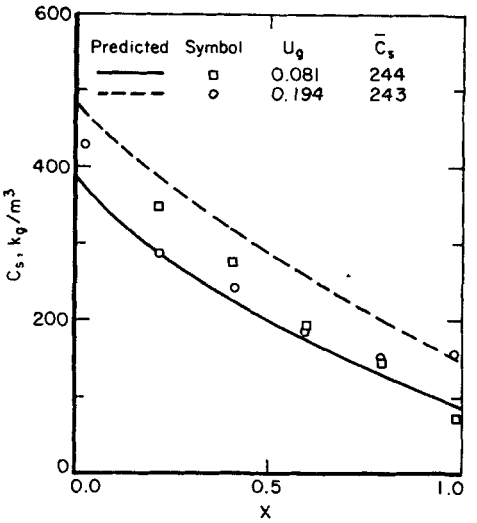

Figure 18. Axial solids concentration as a function of gas velocity (unbaffled column).

outlier, shows that C_s^l is 23% higher than C_s^f,which is in close agreement with Smith and Ruether.

The results of C_s^l as a function of C_s^f for the baffled column and the unbaffled columns obtained in the present study are shown in Figure 15. The data for the baffled column indicate that C_s^l is approximately equal to C_s^f, and we have equated the two expressions in the following analysis. For the unbaffled column, the correlation, Eq. 25, reported by Smith and Ruether (1985) will be used.

$$C_s^l = 1.27\, C_s^f \tag{25}$$

Axial solids concentration distribution: dependence on operating conditions

The prediction of axial solids concentration distributions is made with the sedimentation-dispersion model and the above-mentioned empirical expression for ϵ_g, U_p, E_s, and C_s^l. A comparison of the measured and predicted axial solids concentration distributions in an unbaffled and baffled column for different average solids concentration is shown in Figures 16 and 17. Agreement between observed and predicted distributions is good. The variance in the solids concentration profile, as indicated by the relative change in solids concentration between the bottom and top of the column, is greater for the lower average solids concentration. This is expected from the decrease in hindered settling velocity with an increase in average solids concentration in the slurry.

The dependence of axial solids concentration distributions on superficial gas velocity for the unbaffled column and the baffled column is shown in Figures 18 and 19, respectivley. Higher gas velocities slightly decrease the variance in the axial solids concentration distribution. The predicted and observed profiles are in relatively good agreement for the baffled column. For the unbaffled column the shape of the axial solids distribution is accurate; however, the prediction of $\bar{C}_s$ is not.

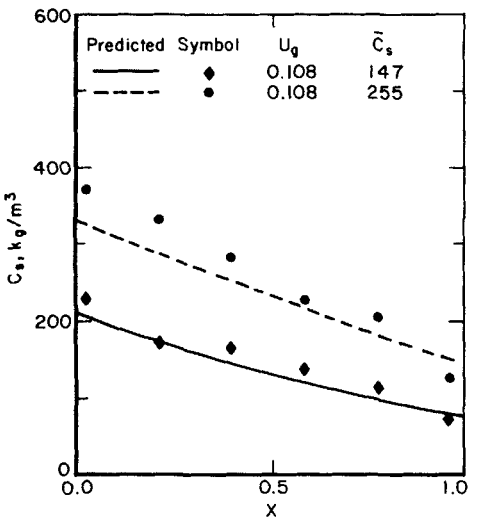

Figure 17. Axial solids concentration as a function of solids loading (baffled column).

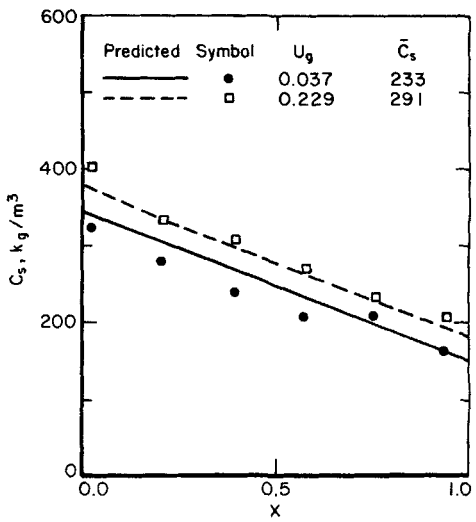

Figure 19. Axial solids concentration as a function of gas velocity (baffled column).

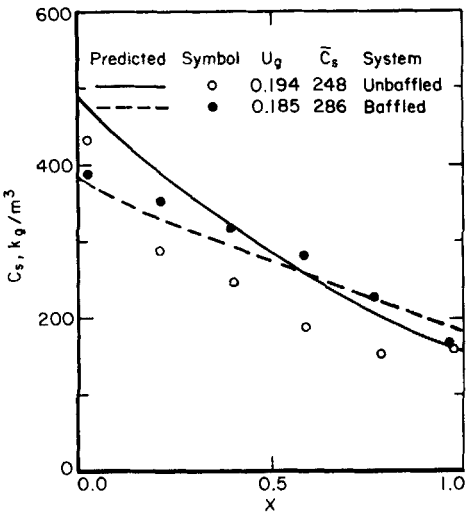

Figure 20. Axial solids concentration distributions for unbaffled and baffled columns.

At similar operating conditions, the axial solids concentration distributions are compared for unbaffled and baffled columns in Figures 20 and 21. Figure 20 compares the profiles obtained at high velocities. Here, the baffled column provides a more uniform solids concentration profile than the unbaffled column. As shown in Figure 21, at low velocities the baffled column provides a more uniform axial solids concentration profile than the unbaffled column. As discussed earlier, this is a result of a lower U_p/E_s ratio in the baffled column, which results in a more uniform profile compared to the unbaffled column.

The use of baffles in a slurry column in general provides a more uniform axial solids concentration distribution than an unbaffled column for otherwise similar operating conditions. The effect is more pronounced at lower gas velocities (less than 0.10 m/s). This is a result of increased mixing and reduced hindered settling velocities when baffles are present.

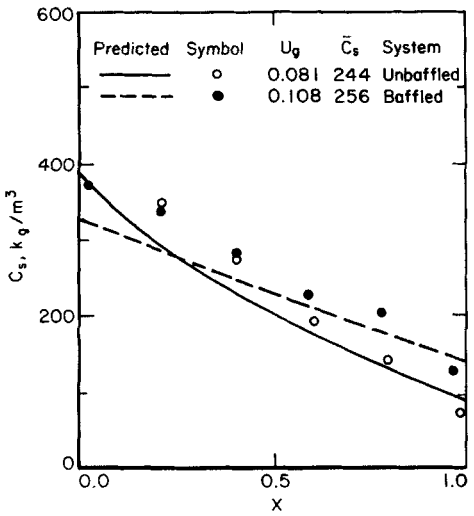

Figure 21. Axial solids concentration distributions for unbaffled and baffled columns.

Discussion

It is important to understand the effect of internal baffles on the slurry bubble column environment for proper scale-up and design of Fischer-Tropsch slurry reactors. The vertical baffle arrangement shows an influence on both the gas and solid phase characteristics measured in the slurry bubble column operated in the churn-turbulent flow regime.

The measured bubble size and gas holup are affected by both the presence of baffles and the solids concentration. Increasing the solids concentration results in large bubble sizes and lower gas holdups for both column configurations. Increasing solids concentration results in increased viscosity, which promotes coalescence resulting in large bubbles. The increased bubble size is associated with increased rise velocities and therefore lower holdups. Interfacial area calculated from the measured gas holdup and bubble size is of the utmost importance in determining the mass transfer resistance. The interfacial area is larger in the baffled column at low gas velocities (<0.11 m/s), while the reverse is true at higher gas velocities. This is a direct result of the bubble size measurement and needs to be investigated further.

Expressions for the solids concentration at the top of the column, for the hindered settling velocity, and for the solids dispersion coefficient are developed to describe the axial solids concentration profile. The solids concentration at the top of the column is similar to the feed concentration for the baffled column. In the unbaffled column, however, the solids concentration at the top of the column is greater than the feed concentration. Hindered settling velocity U_p is shown to be affected by the gas velocity, solids concentration, and the presence of baffles. Two expressions are developed for the unbaffled and baffled column that show the hindered settling velocity decreases by approximately 15% in the presence of baffles at comparable gas velocities and solids concentration. The solids dispersion coefficient E_s is shown to be affected by the gas velocity and the presence of baffles. Two expressions are developed which show that the solids mixing intensity is greater in a baffled column than in an unbaffled column at comparable operating conditions.

The ratio of the hindered settling velocity to solids dispersion coefficient U_p/E_s indicates the uniformity of the axial solids concentration, with a smaller U_p/E_s indicating a more uniform profile. The baffled column in general displays lower U_p/E_s ratios than the unbaffled column, and this result is more pronounced at lower gas velocities.

Acknowledgement

The authors thank Donn Smith and Charles Brodd for conducting all the experimental measurements, and Robert Hamilton and Lynn Billanti for drafting the figures. This research was supported in part by an appointment to the U.S. Department of Energy Postgraduate Research Training program administered by Oak Ridge Associated Universities.

Notation

a = interfacial area, m^{-1}
C = concentration, kg/m^3
D = effective column diameter, Eq. 4, m
D_r = rod diameter, m
d_p = particle diameter, m
d_{vs} = Sauter mean bubble diameter, m
E_s = solids dispersion, m/s
F = objective function, Eq. 10
Fr_g = Froude number, $U_g/(gD)^{1/2}$

g = gravitational acceleration, m/s^2
h = axial distance between probes, m
i = ith measurement
L = length of bubble column, m
M = power law exponent, Eq. 3
n = number of rods in column
N = power law exponent, Eq. 2
Pe_p = Peclet number, $U_g D/E_s$
r = effective radial distance from center of bubble column, m
R = effective radius of bubble column, m
r^* = dimensionless radial position, r/R
Re_g = gas Reynolds number, $U_g D\rho_L/\mu_L$
Re_p = particle Reynolds number, $d_p\rho_L U_t/\mu_L$
ΔT = lag time, s
U_{bo} = bubble terminal rise velocity, m/s
U_g = superficial gas velocity, m/s
U_o = drift velocity, m/s
U_p = hindered settling velocity, m/s
U_{sL} = superficial slurry velocity, m/s
U'_{sL} = slurry velocity, m/s
U_t = terminal settling velocity of single particle, m/s
X = dimensionless axial position

Greek letters

ϵ_g = gas holdup fraction
μ = viscosity, $Pa \cdot S$
ψ = volume fraction in slurry
ρ = density, kg/m^3
ϕ_s = volume fraction of solids in slurry
τ = dwell time, s
λ = bubble length, m

Subscripts

c = center
g = gas
s = solids
L = liquid
sL = slurry
w = wall

Superscripts

$-$ = average
f = feed
1 = top of the column

Literature Cited

Ahrendts, J., and H. Baehr, "The Use of Nonlinear Regression Processes in Establishing Thermodynamic Equations of State," *Int. Chem. Eng.*, **21,** 572 (1981).

Badgujar, M. N., Y. T. Shah, D. N. Smith, and J. A. Ruether, "Solids Distribution in Bubble Column with Liquid Mixtures," *Chem. Eng. Commun.* (1986).

Burgess, J. M., and P. H. Calderbank, "The Measurement of Bubble Parameters in Two Phases. I," *Chem. Eng. Sci.*, **30,** 743 (1975).

Capuder, E., and T. Koloini, "Gas Holdup and Interfacial Area in Aerated Suspensions of Small Particles," *Chem. Eng. Res. Dev.*, **62,** 255 (1984).

Cova, D. R., "Catalyst Suspension in Gas-Agitated Tubular Reactors," *Ind. Eng. Chem., Process Des. Dev.*, **5,** 20 (1966).

Deckwer, W.-D., "F-T Process Alternatives Hold Promise," *J. Oil and Gas,* 198 (1980).

Deckwer, W.-D., Y. Serpemen, M. Ralek, and B. Schmidt, "Modeling the Fischer-Tropsch Synthesis in the Slurry Phase," *Ind. Eng. Chem., Process Des. Dev.*, **21,** 231 (1982).

Fajner, D., F. Magelli, M. Nocenti, and G. Pasquali, "Solid Concentration Profiles in a Mechanically Stirred and Staged Column Slurry Reactor," *Chem. Eng. Res. Dev.*, **63,** 236 (1985).

Fuchs, W., and D. N. Smith, "Conductivity Probe and Data Acquisition for a Liquefaction Cold Model," *Proc. Symp. Instrumentation and Control for Fossil Energy Processes,* ANL-82-62, 223, Houston (1982).

Haberman, W. L., and R. K. Morton, "An Experimental Investigation of the Drag and Shape of Air Bubbles Rising in Various Liquids," David W. Taylor Model Basin Rep. 802 (1953).

Heijner, J. J., and K. van't Riet, "Mass Transfer, Mixing, and Heat Transfer Phenomena in Low-Viscosity Bubble Column Reactors," *Chem. Eng. J.*, **28,** B21 (1984).

Hess, M., "Alternate Distribution Functions of Bubble Diameters Log Normal and Log Gamma Distribution Functions," Final Report DE-AP22-83PC10614 (July, 1983).

Hills, J. H., "Radial Nonuniformity of Velocity and Voidage in a Bubble Column," *Trans. Inst. Chem. Eng.*, **52,** 1 (1974).

Joshi, J. B., "Axial Mixing in Multiphase Contractors—A Unified Correlation," *Trans. Inst. Chem. Eng.*, **58,** 155 (1980).

Kara, S., B. G. Kelkar, Y. T. Shah, and N. L. Carr, "Hydrodynamics and Axial Mixing in a Three-Phase Bubble Column," *Ind. Eng. Chem., Process Des. Dev.*, **21,** 584 (1982).

Kato, Y., A. Nishiwaki, T. Fukuda, and S. Tanaka, "The Behavior of Suspended Solid Particles and Liquid in Bubble Columns," *J. Chem. Eng. Japan,* **5,** 14 (1972).

Kato, Y., A. Nishiwaki, T. Kago, T. Fukuda, and S. Tanaka, "Gas Holdup and Overall Volumetric Absorption Coefficient in Bubble Columns with Suspended Solid Particles. Absorption Rate of Oxygen by an Aqueous Solution of Sodium Sulfite," *Int. Chem. Eng.*, **13,** 562 (1973).

Kato, Y., A. Nishiwaki, S. Tanaka, and T. Fukuda, "Longitudinal Concentration Distribution of Suspended Solid Particles in Multistage Bubble Columns," *J. Chem. Eng. Japan,* **15,** 376 (1982).

Koide, K., A. Takazawa, M. Komura, and H. Matsuraga, "Gas Holdup and Volumetric Liquid-Phase Mass Transfer Coefficient in Solid-Suspended Bubble Columns," *J. Chem. Eng. Japan,* **17,** 459 (1984).

Kölbel, H., and M. Ralek, "The Fischer-Tropsch Synthesis in the Liquid Phase," *Catal. Rev.-Sci. Eng.*, **21** 225 (1980).

Muroyama, K., Y. Mitani, and A. Yasunishi, "Hydrodynamic Characteristics and Gas-Liquid Mass Transfer in a Draft Tube Slurry Reactor," *Chem. Eng. Commun.*, **34,** 87 (1985).

Nassos, G. P., and S. G. Bankoff, "Slip Velocity Ratios in an Air-Water System Under Steady State and Transient Condition," *Chem. Eng. Sci.*, **22,** 661 (1966).

Nicklin, D. J., "Two-Phase Bubble Flow," *Chem. Eng. Sci.*, **17,** 693 (1962).

Peebles, R. N., and H. J. Garber, "Studies of Motion of Gas Bubbles in Liquid," *Chem. Eng. Prog.*, **49,** 88 (1953).

Quicker, G., A. Schumpe, and W.-D. Deckwer, "Gas-Liquid Interfacial Areas in a Bubble Column with Suspended Solids," *Chem. Eng. Sci.*, **39,** 179 (1984).

Riquarts, H.-P., "A Physical Model for Axial Mixing of the Liquid Phase for Heterogeneous Flow Regime in Bubble Columns," *Ger. Chem. Eng.*, **4,** 18 (1981).

Roy, N. K., D. K. Guha, and M. N. Rao, "Fractional Gas Holdup in Two-Phase and Three-Phase Batch Fluidized Bubble-Bed and Foam-Bed Systems," *Indian Chem. Eng.*, **27** (1963).

Shah, Y. T., C. A. Ratway, and H. G. McIluried, "Backmixing Characteristics of a Bubble Column with Vertically Suspended Tubes," *Trans. Inst. Chem. Eng.*, **56,** 107 (1978).

Shah, Y. T., B. G. Kelkar, S. P. Godbole, and W.-D. Deckwer, "Design Parameters Estimation for Bubble Column Reactors," *AIChE J.*, **28,** 353 (1982).

Shah, Y. T., S. Joseph, D. N. Smith, and J. A. Ruether, "Two-Bubble Class Model Churn-Turbulent Bubble Column Reactor," *Ind. Eng. Chem., Process Des. Dev.*, **24,** 1096 (1985a).

———, "On the Behavior of Gas Phase in a Bubble Column with Ethanol-Water Mixtures," *Ind. Eng. Chem., Process Des. Dev.*, **24,** 1140 (1985b).

Smith, D. N., W. Fuchs, R. J. Lynn, D. H. Smith, and M. Hess, "Bubble Behavior in a Slurry Bubble Column Reactor," *Am. Chem. Soc. Symp. Ser.* 237, *Chemical and Catalytic Reactor Modeling,* M. P. Dudakuic, P. L. Millo, eds., 125 (1984).

Smith, D. N., and J. A. Ruether, "Dispersed Solid Dynamics in a Slurry Bubble Column," *Chem. Eng. Sci.*, **40,** 741 (1985).

Smith, D. N., J. A. Ruether, Y. T. Shah, and M. N. Badgujar, "Modified Sedimentation-Dispersion Model for Solids in a Three-Phase Slurry Column," *AIChE J.*, **32,** 426 (1986).

Suganuma, T., and T. Yamanishi, "Concentration Gradient in Multiple-Stage Gas Bubble Columns," *Kagaku Kogaku,* **30,** 1136 (1966).

Tanaka, S., T. Fukuda, A. Nishiwaki, and Y. Kato, "Residence Time Distribution of Suspended Solid Particles in Multistage Bubble Column," *J. Chem. Eng. Japan*, **17**, 99 (1984).

Towell, G. D., C. P. Strand, and G. H. Ackerman, "Mixing and Mass Transfer in Large-Diameter Bubble Columns," *AIChE-Inst. Chem. Eng. Symp. Ser.*, **10**, 97 (1965).

Tsutsui, T., and T. Miyauchi, "Fluidity of a Fluidized Catalyst Bed and Its Effect on the Behavior of the Bubbles," *Int. Chem. Eng.*, **20**, 386 (1980).

Ueyama, K., and T. Miyauchi, "Properties of Recirculating Turbulent Two-Phase Flow in Gas Bubble Columns," *AIChE J.*, **25**, 258 (1979).

Ueyama, K., S. Morooka, K. Koide, K. Hisatsuyu, and T. Miyauchi, "Behavior of Gas Bubbles in Bubble Columns," *Ind. Eng. Chem., Process Des. Dev.*, **19**, 592 (1980).

van der Welle, R., "Void Fraction, Bubble Velocity, and Bubble Size in Two-Phase Flow," *Int. J. Multiphase Flow*, **11**, 317 (1985).

Walters, J. F., and H. W. Blanch, "Liquid Circulation Patterns and Their Effect on Gas Holdup and Axial Mixing in Bubble Columns," *Chem. Eng. Commun.*, **19**, 243 (1983).

Werther, J., "Bubbles in Gas Fluidized Beds. I," *Trans. Inst. Chem. Eng.*, **52**, 149 (1974).

Yamanaka, Y., T. Sekizawa, and H. Kubota, "Age Distribution of Suspended Solid Particles in a Bubble Column," *J. Chem. Eng. Japan*, **3**, 264 (1970).

Yamashita, F., Y. Mori, and S. Fujita, "Sizes and Dize Distribution of Bubbles in a Bubble Column—Comparison Between the Two-Point Conductivity Probe and the Photographic Method," *J. Chem. Eng. Japan*, **12**, 5 (1979).

Ying, D. H., E. N. Givens, and R. F. Weimer, "Gas Holdup in Gas-Liquid and Gas-Liquid-Solid Flow Reactors," *Ind. Eng. Chem., Process Des. Dev.*, **19**, 635 (1980).

Manuscript received Oct. 22, 1986, and revision received June 14, 1987.